ELSEVIER

Thermal conductivity of highly porous mullite material

Rafael Barea [a], Maria Isabel Osendi [a], Jose M.F. Ferreira [b], Pilar Miranzo [a],*

[a] *Instituto de Cerámica y Vidrio, CSIC, C/Kelsen 5, Campus de Cantoblanco, 28049 Madrid, Spain*
[b] *Department of Ceramics and Glass Engineering, CICECO, Campus Santiago, University of Aveiro, 3810-193 Aveiro, Portugal*

Abstract

The thermal diffusivity of highly porous mullite materials (35–60 vol.% porosity) has been measured up to 1000 °C by the laser flash method. These materials were fabricated by a direct consolidation method based on the swelling properties of starch granules in concentrated aqueous suspensions and showed mainly spherical shaped pores of about 30 μm in diameter. From the point of view of heat conduction, they behave as a bi-phase material of voids dispersed in the continuous mullite matrix. The temperature dependence of thermal conductivity for the different porosities was modeled by a simple equation that considers the contribution to heat conduction of the mullite matrix and the gas inside the pores, as well as the radiation. The thermal conductivity of the matrix was taken from the measurements done in a dense mullite while the conductivity in the voids was assumed to be that of the testing atmosphere.
© 2005 Acta Materialia Inc. Published by Elsevier Ltd. All rights reserved.

Keywords: Thermal conductivity; Porous material; Mullite; Modelling

1. Introduction

Generally, porous materials are used in applications that require low, fixed, and well defined thermal conductivity figures; for instance, in catalyst supports, hot-gas or molten-metal filters, membranes and gas burners [1,2]. Mullite is one of the ceramic materials suitable for these types of uses due to its high temperature strength, as well as its creep resistance [3]. Furthermore, porous mullite bodies have been used for fabricating composite-type components by impregnating mullite foams with polymers, inorganic cements or metals [4]. In this case, thermal conductivity is again a key property.

In spite of the technological interest of highly porous mullite, only a few works regarding its processing methods and none concerning the thermal conductivity have been found in the literature [5–10]. The preparation of porous mullite materials with porosities ranging from 40 to 60 vol.% can be readily achieved by a direct consolidation method based on the swelling properties of starch in water, as described elsewhere [11].

Among the techniques available to measure the thermal conductivity, the laser flash method stands out for its low run time (less than 1 h per temperature) and the reduced sample size required. This method measures the thermal diffusivity, which can be directly related to the thermal conductivity by the equation

$$K = \alpha \cdot C_p \cdot \rho, \tag{1}$$

where α is the thermal diffusivity, C_p is the specific heat and ρ the material's density. This technique is especially suitable for dense and opaque materials but it is not so appropriate for materials transparent to infrared radiation or with pores, since laser radiation can penetrate through the sample. In the case of porous materials, this problem can be overcome by correcting the measured thickness by the pore size as has been discussed in a previous work [12].

---

* Corresponding author. Tel.: +34 917 355 872; fax: +34 917 355 843.
  E-mail address: pmiranzo@icv.csic.es (P. Miranzo).

The aim of the present work is to investigate and model the variations in the thermal conductivity of highly porous mullite materials (up to 60 vol.%) as a function of the percentage of porosity, over a wide range of temperatures.

2. Experimental procedure

Commercial mullite powders (Baikalox-SASM, Baikowsky Chimie, France) and a modified potato starch (Trecomex AET1, Lyckeby Stärkelsen AB, Sweden) have been used as starting materials for this study. Materials have been prepared as described in detail in a previous paper [11]. In short, starch granules (in volume fractions ranging from 0.15–0.55) were added to stable aqueous mullite suspensions containing a total solids loading of 45 vol.%; the slurries were then poured into plastic moulds and gelified in air at 80 °C for 1–3 h; next, de-molding and drying at 40 °C were carried out; the resultant green samples were heated in air at a rate of 4 °C/min up to 700 °C to burn out the organic matter and finally were sintered at 1680 °C for 2 h. A dense mullite specimen (93% of the theoretical density) was also prepared by uniaxial pressing at 85 MPa and sintering at 1680 °C during 2 h, for comparative purposes.

The porosity and density were measured by the Archimedes' method. For calculations, a theoretical density of 3.16 g/cm^3 was used for mullite.

The microstructure of each material was observed on polished and thermally etched (1500 °C/60 min) samples by scanning electron microscopy (SEM). The pore size was determined from SEM micrographs using image analysis techniques [11]. An average of 200 pores was considered for the measurements.

The thermal diffusivity (α) was measured by the laser flash method (Thermaflash 2200, HOLOMETRIX, USA). Tests were performed in an Ar atmosphere up to 1000 °C, on disk shaped samples of 12.7 mm in diameter and 1–2 mm of thickness. Specimen surfaces were gold and graphite coated to enhance absorption of the laser energy. Software based on the Koski's [13] method, which considers heat losses and finite pulse corrections, was used to obtain the diffusivity from the temperature–time runs. Experimental data were corrected considering that the actual thickness was the measured one reduced by twice the maximum surface roughness of the specimens, according to previous studies of the authors [12,14]. This method allows the effect of the pore size in the sample thickness to be taken into account.

Data given in [15] for the specific heat (C_p) of mullite at each temperature were used in Eq. (1) to calculate the thermal conductivity (K). The effect of the temperature dependence of density on the thermal conductivity was not considered as the error associated with it is smaller than the accuracy of the laser flash technique, which is 5% for thermal diffusivity, as is discussed below.

Considering that the thermal dilatation is different in the a, b, and c axis of the mullite unit cell, the real volume, V, at a given temperature T, would be

$$V/V_0 = 1 + T^3[\alpha(a) \cdot \alpha(b) \cdot \alpha(c)] \\ + T^2[\alpha(a) \cdot \alpha(b) + \alpha(b) \cdot \alpha(c) + \alpha(c) \cdot \alpha(a)] \\ + T[\alpha(a) + \alpha(b) + \alpha(c)], \quad (2)$$

where V_0 is the volume at room temperature, and $\alpha(a)$, $\alpha(b)$ and $\alpha(c)$ are the thermal dilatation coefficients along the three axes. The relative error on thermal conductivity associated with this volume change can then be estimated from Eq. (1) as

$$\Delta k/k = |1 - V/V_0| \times 100. \quad (3)$$

Introducing the in situ high temperature lattice parameters given by Schneider and Eberhard [16] for $\alpha(a)$, $\alpha(b)$ and $\alpha(c)$, the relative error ranges between 0.2% and 1.7%, depending on temperature, and therefore it is not relevant for thermal conductivity calculations.

3. Results and discussion

Table 1, which collects the main characteristics of the samples, shows that the surface roughness ranges from 34 to 47 μm, similar to the pore size. Fig. 1 represents thermal conductivity data, with and without the corresponding thickness correction, as a function of temperature for all the samples. It can be observed that experimental data are reduced by ~15% when the correction is made. The material labeled as "0" in Fig. 1 refers to the dense mullite without starch additions. A steady decay in conductivity with temperature is observed for this material, from 4.63 W/m K at room temperature to 3.15 W/m K at 1000 °C, which is the usual behavior in crystalline materials. However, the porous specimens show a more moderate decrease with temperature; in fact, the 57 vol.% porous mullite showed an almost constant thermal conductivity in the whole temperature range, from 1.10 W/m K at 25 °C up to 0.91 W/m K at 1000 °C. The thermal conductivity of the more porous samples is quite significantly lower than

Table 1
Main characteristics of the porous mullite materials

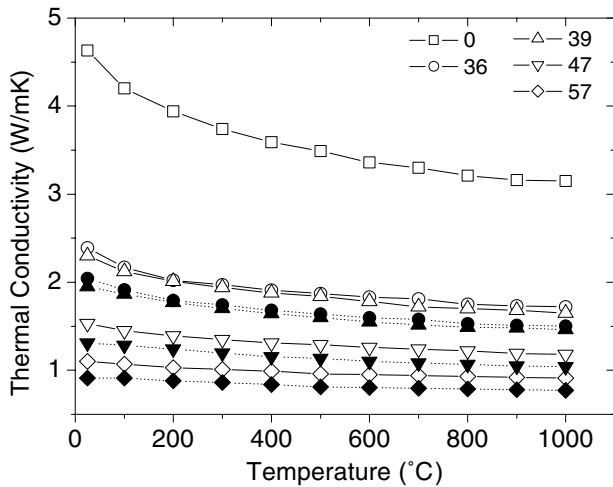| Material	Porosity (%)	Maximum surface roughness (μm)	Mean pore size (μm)	Mean pore aspect ratio
M15	37	38 ± 3	42 ± 27	1.69 ± 0.93
M25	39	39 ± 5	30 ± 16	1.78 ± 0.49
M35	47	34 ± 3	27 ± 14	1.55 ± 0.35
M55	57	40 ± 9	31 ± 21	1.62 ± 0.44

Fig. 1. Thermal conductivity vs. temperature for mullite samples of different porosity percentages (in the legend). Full symbols represent values after the thickness correction (only for porous specimens).

voids match the original starch particles in shape and size. Average pore sizes and pore aspect ratios are gathered in Table 1 for all the samples. According to these microstructures, the porous materials have been treated as a composite of two phases having different thermal conductivities, corresponding to the mullite matrix and the voids. The simple expression developed by Eucken [17] for dilute dispersed particles was applied, though this model is only valid for second phase contents below the percolation limit (∼15 vol.% [18]):

$$K_{ef}/K_0 = 1 + 2\chi - 2V(\chi - 1)/1 + 2\chi + V(\chi - 1), \qquad (4)$$

with K_{ef} being the effective conductivity of the composite, K_0 the thermal conductivity of the continuous phase and $\chi = K_0/K_{Inclusion}$, where $K_{Inclusion}$ is the conductivity of the discontinuous phase and V is its volume fraction.

In the present case, the thermal conductivity of the continuous phase was taken as that measured for the near dense mullite material corrected to zero porosity using Klemens' equation [19]

$$K_0'/K_0 = 1 - 4/3V, \qquad (5)$$

where K_0' is the thermal conductivity measured for the nominal dense material (7% of porosity) and K_0 is that value corrected to zero porosity. The value of K_0 at 25 °C is 5.1 W/m K. There are scarce data in the literature for

the dense sample; e.g., a 76% lower value is measured at 25 °C for the 57 vol.% porous sample.

The microstructure of the porous mullite specimens (Fig. 2) can be regarded as consisting of a continuous mullite matrix with spherical void inclusions of 30–42 μm in diameter and a mean aspect ratio of ∼1.6. The
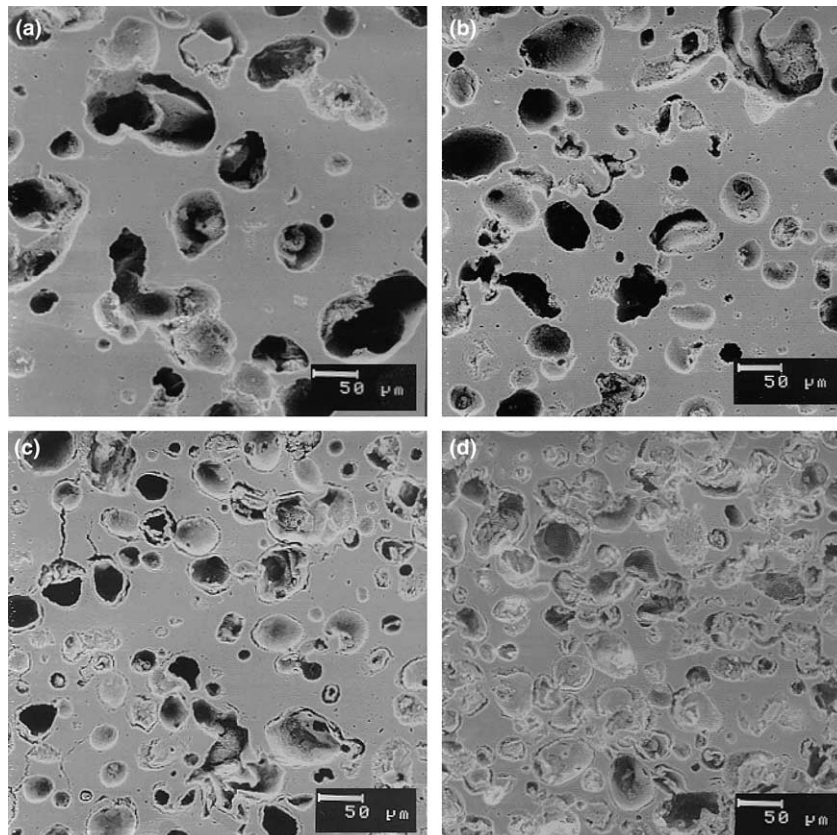

Fig. 2. SEM micrographs of the porous mullite specimens with (a) 36, (b) 39, (c) 47 and (d) 57 vol.% of porosity.

the thermal conductivity of dense mullite materials. Among them we can name those reported in CRC Materials science and engineering handbook [20] and Kingery et al. [17], which in fact give the same values (∼6 W/m K at 100 °C) from a source [21] of 1964. Nevertheless, no data about the thermal conductivity method and the microstructure of the specimen are given there and therefore, they cannot be meaningful compared with the K data presented here. On the other hand, more recent works [22,23] show similar values, also measured by the laser flash method, to those of the present paper: 5.2 and 5.7 W/m K at 25 °C for dense mullite bodies processed from alkoxide mullite [22] and high purity mullite powders [23], respectively. Furthermore, taking into account the range of thermal conductivity values given for dense mullite, new studies, more exhaustive in relation to the microstructure, should be done in order to get more reliable data.

As thermal diffusivity measurements were done in an argon atmosphere and therefore voids were filled with this gas, the thermal conductivity of the dispersed phase in Eq. (4) is assumed to be that of argon. Thermal conductivity of Ar as a function of temperature was calculated by the least squares fitting of tabulated data given in [24] to the following equation:

$$K_{Argon} = 0.0017T^{0.5} - 0.0112, \tag{6}$$

where a $T^{0.5}$ dependence was assumed based on the kinetic theory of gases [25].

Although the effective thermal conductivity data do not match the Eucken's equation (Fig. 3), the fit is better than could be expected considering that this equation is a quite simple approximation only valid for dilute media. Probably, this approximation is not unrealistic because void percolation was not observed, even for the

highest porosity (Fig. 2). A better fit is attained if the empirical weight function proposed by Singh et al. [26] for systems with two phases of quite different thermal conductivities and a high volume fraction of the dispersed phase is used to modify the Eucken's expression. In this way, the volume fraction of pores in Eq. (4) is replaced by the factor

$$F_2 = 1 - \exp\left\{-0.92V^2 \log\frac{K_{Argon}}{K_0}\right\}, \tag{7}$$

which gives the effective thermal conductivity vs. porosity curves plotted in Fig. 3 as discontinuous lines. Although experimental data at room temperature match this curve, data at 800 °C diverge from its corresponding fit.

Regarding the thermal conductivity–temperature behavior, K of the dense mullite is readily fitted to the following equation (Fig. 4):

$$K_0 = 23.2T^{-0.27}. \tag{8}$$

However, it was impossible to obtain similar good fits using a $T^{-0.27}$ dependence for the porous materials. Hence, to model this behavior the intention was to develop a simple equation that clearly shows the relative contribution of each phase. First, let us consider the effective thermal conductivity of the porous material as given by

$$\frac{1}{K_{ef}(T)} = \frac{P_1(V)}{K_0(T)} + \frac{P_2(V)}{K_{Argon}(T)}, \tag{9}$$

where $P_1(V)$ and $P_2(V)$ are functions of porosity and $K_0(T)$ and $K_{Argon}(T)$ represent the temperature dependence of thermal conductivity for the dense mullite ($T^{-0.27}$ from Eq. (8)) and the gas phase ($T^{0.5}$ from Eq. (6)), respectively. This mathematical law means that the contribution of the atmosphere to the temperature
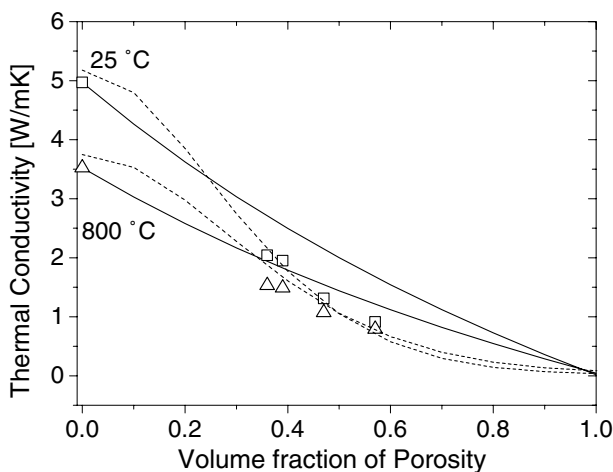

Fig. 3. Thermal conductivity as a function of porosity for all the mullite specimens tested at two different temperatures. Continuous lines represent values from Eq. (4) and dashed lines data corrected using Eq. (7).
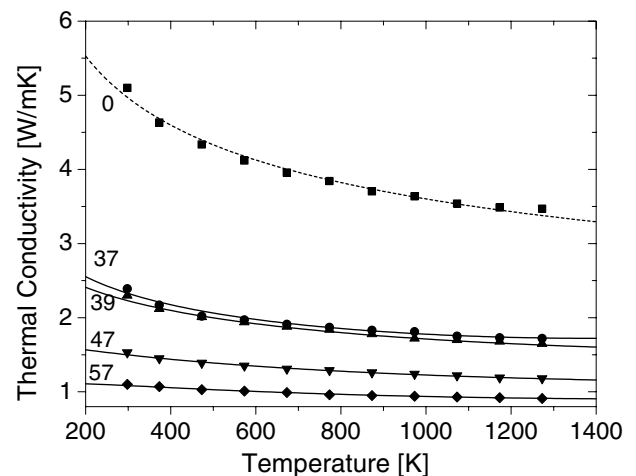

Fig. 4. Temperature dependence of thermal conductivity for the porous and dense specimens. Discontinuous line corresponds to values given by Eq. (8) and continuous lines to those given by Eq. (10).

dependence of the thermal conductivity of porous materials can be considered by introducing in a rule of mixtures a weight function dependent on the fraction porosity.

Replacing $K_0(T)$ and $K_{\mathrm{Argon}}(T)$ in Eq. (9), K_{ef} as a function of temperature can be obtained

$$K_{\mathrm{ef}}(T) = \frac{T^{0.23}}{P_2(V)T^{-0.27} + P_1(V)T^{0.5}} + P_3 T^3. \qquad (10)$$

The term $P_3 T^3$ that weights the contribution of radiation to the conductivity is also added. The parameters P_1, P_2 and P_3 were estimated by the least squares fitting of this equation to the experimental data. The fitting achieved for each material is represented in Fig. 4 by a solid line, showing a very good agreement with experimental data. In Fig. 5, the calculated parameters P_1 and P_2 are plotted as a function of porosity. The higher slope observed for P_2 seems to indicate that the contribution of the $T^{0.5}$ term is more important for higher porosity volumes and leads to a softer dependence of the thermal conductivity on the temperature. From this figure, it is evident that the model cannot be applied for porosities below 35% as P_2 becomes negative.

If we represent P_3 data as a function of the average pore diameter of each specimen, a linear dependence is clearly observed (Fig. 6), as theory predicts. Actually, the radiation contribution to the thermal conductivity in porous materials can be estimated by the expression [17]

$$K_{\mathrm{rad}} = 4\sigma_{\mathrm{B}}\varepsilon n^2 dT^3, \qquad (11)$$

in which σ_{B} is the Stefan–Boltzmann constant, ε the emissivity, n the refraction index and d is the pore diameter. Assuming $\varepsilon \sim 1$, n as the argon refraction index (~ 1) and d as the measured mean pore size (27–42 μm in Table 1), a value of $\sim 1 \times 10^{-11} T^3$ W/m K is estimated for K_{rad}. This value is very close to that deduced from the proposed equation that is in the range $1 \times 10^{-11} T^3$ to $5 \times 10^{-11} T^3$ W/m K.
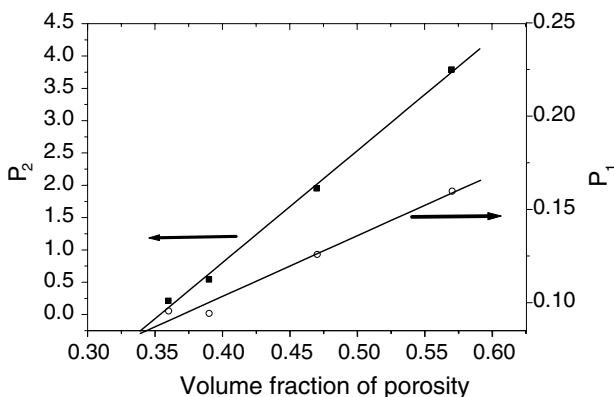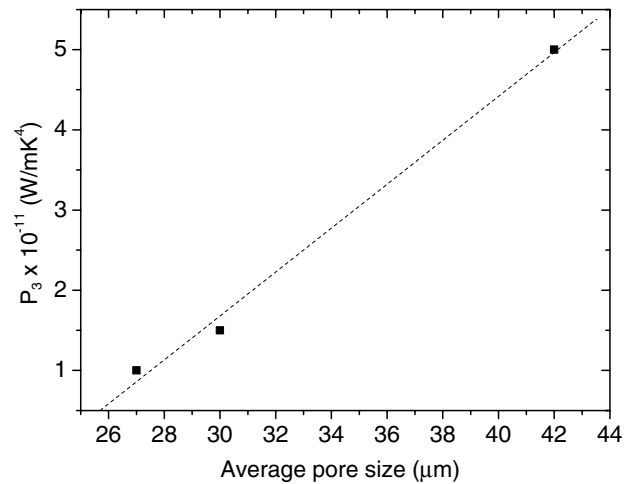

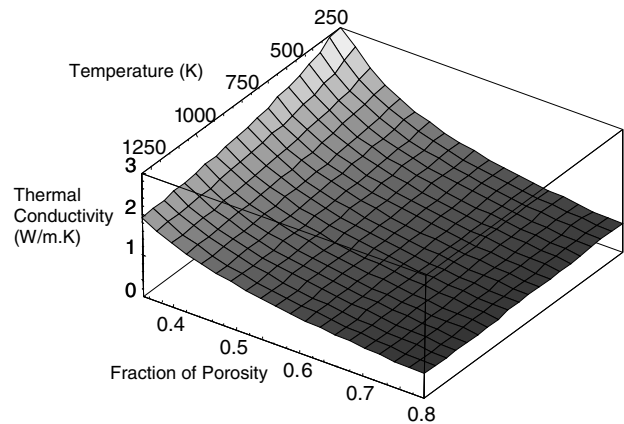Fig. 6. Parameter P_3 as a function of the average pore size for the different porous mullites.

Fig. 7. Effective thermal conductivity vs. temperature and porosity fraction as predicted by Eq. (10) for porous mullite.

The dependence of $K_{\mathrm{ef}}(T,V)$ with porosity and temperature as predicted by Eq. (10) for porous mullite specimens is jointly depicted in Fig. 7. Using this expression we can predict the volume of pores required to get a given thermal conductivity in a mullite body.

4. Conclusions

From the point of view of the heat conduction, porous mullite (porosity in the range $\sim$35 to 60 vol.% and pore sizes $\sim$40 μm) behaves as a bi-phase material of voids dispersed in the continuous and dense mullite matrix. The thermal conductivity of materials with porosities $\geqslant$45% is almost constant with temperature and $\sim$75% lower than that of the dense mullite.

A simple equation that models the temperature dependence of thermal conductivity for the different porosities has been proposed, which includes the

Fig. 5. Parameters P_1 and P_2 as a function of porosity.

contribution to heat conduction of the dense mullite matrix and the gas inside pores, as well as radiation.

Acknowledgments

References

[1] Saggio-Woyansky J, Scott C, Minnear WP. Am Ceram Soc Bull 1992;71(11):1674–82.
[2] Sheppard LM. Porous ceramic processing and applications. In: Ishizaki K, Sheppard LM, Okada S, Hamasaki T, Huybretzhts B, editors. Ceramic transactions. Porous materials, vol. 31. Westerville (OH), USA: American Ceramic Society; 1993. p. 3–23.
[3] Schneider H, Okada K, Pask JA. Mullite and mullite ceramics. New York (NY): John Wiley & Sons; 1994.
[4] Loehman RE, Ewsuk K, Tomsia AP. J Am Ceram Soc 1996;79(1):27–32.
[5] Abe H, Seki H, Fukunaga A, Egashira M. J Mater Sci 1994;29(5):1222–6.
[6] Hashishin T, Joyama A, Kaneko Y. J Ceram Soc Jpn 1998;106(2):127–30.
[7] Miao X. Mater Lett 1999;38(2):167–72.
[8] Atisivan R, Bose S, Bandyopadhyay A. J Am Ceram Soc 2001;84(1):221–3.
[9] Liu YF, Liu XQ, Wei H, Meng GY. Ceram Int 2001;27(1):1–7.
[10] She JH, Ohji T. Mater Chem Phys 2003;80(3):610–4.
[11] Barea R, Osendi MI, Ferreira JMF, Miranzo P. J Am Ceram Soc 2005;88(3):777–9.
[12] Garcia E, Osendi MI, Miranzo P. J Appl Phys 2002;92(5): 2346–2349.
[13] Koski JA. Improved data reduction methods for laser pulse diffusivity determination with the use of minicomputers. In: Proceedings of the eighth symposium on thermophysical properties, vol. II, Gaithersburg, MD, USA. New York (NY): ASME; 1981. p. 94.
[14] Barea R. Thermal conductivity of biphasic ceramics. PhD thesis. Universidad Autónoma de Madrid, Spain; 2004.
[15] Hildmann B, Schneider H. J Am Ceram Soc 2004;87(2):227–34.
[16] Schneider H, Eberhard E. J Am Ceram Soc 1990;73(7):2073–6.
[17] Kingery WD, Bowen HK, Uhlmann DR. Introduction to ceramics. 2nd ed. New York (NY): John Wiley & Sons; 1976.
[18] Kirkpatrick S. Rev Mod Phys 1973;45(4):574–88.
[19] Klemens PG. High Temp–High Press 1991;23:241–8.
[20] Shackelford JF, Alexander W, Park JS, editors. CRC Materials science and engineering hanbook. 2nd ed. Boca Raton (FL), USA: CRC Press; 1994. p. 287.
[21] Shaffer TB, editor. Materials index. Handbook of high temperature materials, vol. 1. New York (NY): Plenum Press; 1964. p. 407–8.
[22] Russell LM, Johnson LF, Hasselman DPH. J Am Ceram Soc 1987;70(10):C226–9.
[23] Kyaw MT, Okamoto Y, Hayashi K. J Ceram Soc Jpn, Int Edn 1995;103(12):1278.
[24] Lide DR, editor. CRC Handbook of chemistry and physics. 84th ed. Boca Raton (FL): CRC Press; 2003.
[25] Levine IN. Physical chemistry. Maidenhead: McGraw-Hill Education; 2001.
[26] Singh KJ, Singh R, Chaudhary DR. J Phys D: Appl Phys 1998;31(14):1681–7.